Liquid Crystals
Publication details, including instructions for authors and subscription information:
http://www.informaworld.com/smpp/title~content=t713926090

Dielectric studies of different phases of a thin-layered ferroelectric liquid crystal with a small pitch and high spontaneous polarization

S. L. Srivastava[a]; V. K. Agrawal[a]; M. V. Loseva[b]; N. I. Chernova[b]; L. A. Beresnev[c]
[a] Department of Physics, University of Allahabad, Allahabad, India [b] Organic Intermediate & Dyes Institute, Moscow, U.S.S.R. [c] AV Shubnikov Institute of Crystallography, U.S.S.R. Academy of Sciences, U.S.S.R.

To cite this Article Srivastava, S. L. , Agrawal, V. K. , Loseva, M. V. , Chernova, N. I. and Beresnev, L. A.(1992) 'Dielectric studies of different phases of a thin-layered ferroelectric liquid crystal with a small pitch and high spontaneous polarization', Liquid Crystals, 11: 6, 851 — 864
To link to this Article: DOI: 10.1080/02678299208030690
URL: http://dx.doi.org/10.1080/02678299208030690

LIQUID CRYSTALS, 1992, VOL. 11, NO. 6, 851–864

Dielectric studies of different phases of a thin-layered ferroelectric liquid crystal with a small pitch and high spontaneous polarization

by S. L. SRIVASTAVA*†, V. K. AGRAWAL†, M. V. LOSEVA‡, N. I. CHERNOVA‡ and L. A. BERESNEV§

† Department of Physics, University of Allahabad, Allahabad 211002, India

‡ Organic Intermediate & Dyes Institute, B Sadovaya, 1–4 Moscow 103787, U.S.S.R.

§ AV Shubnikov Institute of Crystallography, U.S.S.R. Academy of Sciences, 117333 Moscow, Lenninsky Prospekt, 59, U.S.S.R.

(*Received 12 February 1990; accepted 11 December 1991*)

Dielectric spectroscopy of a ferroelectric liquid crystal with planar texture in the frequency range 100 Hz to 1 MHz has been carried out as a function of temperature from 25°C to 60°C at different DC fields varying from 0 to 12 kV cm^{-1}. From the measured dielectric strengths and relaxation frequencies, it is observed that the material has a S_C^*–S_A^* transition at 56·1°C and a S_A^*–I transition at 58°C. The data of the S_C^* phase have been assigned to the Goldstone mode. The rotational viscosity and elastic constant have been calculated from the observed data. The capacitance shows an abrupt drop at the critical DC field where unwinding of the helix occurs. The measured value of the critical field decreases with temperature and agrees to literature data from electrooptical experiments. On applying a DC field greater than 6·5 kV cm^{-1} at room temperature, the liquid crystal shows the unwound S_C^* and S_A^* phases.

1. Introduction

The complex dielectric permittivity of a ferroelectric liquid crystal can be directly measured by dielectric spectroscopic techniques. With the emergence of enhanced accuracies of computer controlled bridges, it is possible to acquire dielectric permittivity and dielectric loss data rather quickly over a wide frequency range at very small frequency steps. The dielectric spectroscopy of a large number of ferroelectric liquid crystals have been recently reported and possible information about the molecular orientation and the relaxation processes have been discussed [1–10]. The planar oriented ferroelectric liquid crystal exhibits the chiral smectic C S_C^* phase over a wide temperature range; the dielectric behaviour of this phase is described to two relaxation processes [1, 9]. The dominant Goldstone mode appears because of the fluctuations of the phase in the azimuthal orientation of the director, whereas the soft mode appears due to the fluctuations in the amplitude of the tilt angle θ. The dielectric relaxation frequencies of the Goldstone mode are weakly dependent on the temperature and are usually lower than 500 Hz [9]. The soft mode in the S_C^* phase could be resolved from the Goldstone mode by only a few tenths of a degree below the S_C^*–S_A^*

* Author for correspondence.

0267-8292/92 $3·00

transition temperature [9]. The relaxation frequencies of the soft mode in the S_C^* phase decrease critically with temperature. The relaxation frequencies in the soft mode are suppressed by the dominant Goldstone mode well below the transition temperature because the dielectric strength of the soft mode is too low to be extracted from that of the Goldstone mode. On heating, the ferroelectric materials undergo the S_C^*–S_A^* transition. In the S_A^* phase only the soft mode is present. The dielectric strength of the soft mode decreases and the relaxation frequency increases with temperature; a feature which is opposite to the temperature behaviour of the soft mode of the S_C^* phase [9]. The temperature interval of the S_A^* phase is typically a few degrees, above the temperature at which the material goes into the isotropic phase.

A static electric field applied perpendicular to the helical axis of the S_C^* phase loosens the stability of the spiral structure. In the limiting strong field, the dipole moments align along the field and the twisted S_C^* phase becomes unwound [11, 12]. The critical field for unwinding the helix depends on the dielectric anisotropy, the tilt angle and the pitch as well as the elastic and piezo- and flexo-coefficients of the material [10]. The static electric field is also, therefore, an important experimental variable for the dielectricity of ferroelectric materials.

For the purpose of electrooptical application a ferroelectric liquid crystal should be in the S_C^* phase at room temperature and should have a large spontaneous polarization, a small pitch and a large relaxation frequency of the Goldstone mode. With this objective in mind the dielectric relaxation studies of some multicomponent ferroelectric liquid crystal mixtures have been recently reported [2, 5, 6, 9]. Electrooptical studies of the mixture FLC#202 with a room temperature S_C^* phase and high spontaneous polarization have been reported earlier [13, 14]. The basic components of this mixture are given in table 1. Here we report the dielectric properties of the material FLC#202 in the frequency range 100 Hz to 1 MHz as a function of temperature (25°C–60°C) at different external DC fields (0–12 kV cm^{-1}) (the elastic constant and the rotational viscosity have been determined from the existing theoretical model).

2. Experimental

The ferroelectric liquid crystal FLC#202 was sandwiched between two conducting glass plates whose surfaces had been treated to obtain planar orientation [13]. A gap of 5·3 μm provided by two teflon strips was filled with the material in its isotropic phase,

Table 1. Basic constituents of FLC#202.

No.	Chemical formula	Ratio by weight	
1.	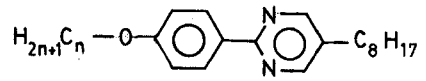	$n=8$ $=9$ $=10$	24·4% 15·6% 22·6%
2.	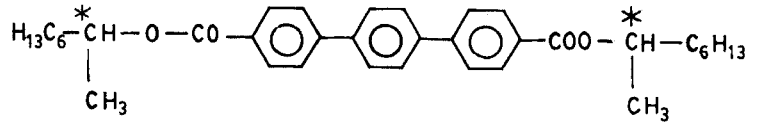		36·9%
3.	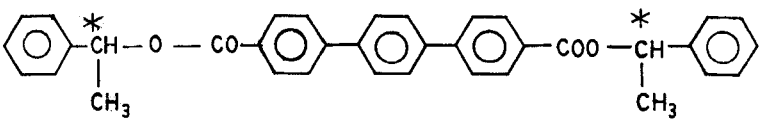		0·5%

which was then cooled slowly to room temperature. The helical structure was observed to be stable under the polarizing microscope. Electrooptic studies on this sample gave the following properties: (i) S_C^* 58°C I, (ii) a spontaneous polarization, P_s 70 nC cm^{-2} at 25°C with a helical pitch of about 0·3–0·4 μm, (iii) a critical field of about 5·6 kV cm^{-1} showed the unwinding of the helix from the molecular tilt experiment and (iv) the molecular tilt angle with respect to the smectic layer normal decreased with increase in temperature [13, 14]. The area of the parallel plate was estimated from the polarizing microscope to be 0·11 cm^2.

A Hewlett–Packard impedance analyser HP4194A working in the 100 Hz to 100 MHz frequency range along with a data acquisition HP300 computer system was used for the dielectric measurements. The oscillator level was kept at 500 mV for all the measurements. The computer program for the measurement of the capacitance, $C(f)$, parallel to the conductance, $G(f)$, at the frequency, f, was run at 401 points of the frequency at equal intervals on the log scale. The frequency of measurement on this sample was limited to 1 MHz. The bridge had the capability of applying fixed or swept DC field bias at spot frequencies. This was used to apply the bias up to 6 V (the corresponding electric field is about 12 kV cm^{-1}) at spot frequencies from 100 Hz to 1 MHz. A thermostatic bath for controlling the temperature was employed. The temperature in the close vicinity of the sample was read by a thermocouple. The temperature accuracy was better than $\pm$0·1°C. The data were taken between 25°C to 60°C since the sample goes into the isotropic phase at 58°C. Though this bridge made it feasible to take data up to 100 MHz, the upper frequency limit of 1 MHz was chosen to avoid the effect of the lead inductance. Moreover, the finite conductivity of the conducting glass electrodes and the fact that the material exhibits extremely low loss in the MHz region make the measurements beyond 1 MHz unrealistic.

The ferroelectric materials show large hysterisis effects with temperature and electric field and, therefore, care had to be taken to minimize them. To avoid the hysterisis due to the external electric field, the measurements of $C(f)$ and $G(f)$ were carried out in the swept log frequency mode at the chosen DC bias in the temperature range of interest. Only the temperature was varied without changing the DC bias. The measurements were also carried out in the swept DC bias mode at spot frequencies on varying the temperature. It was found that the hysterisis effects were not removed completely but one set of observations taken by changing either the temperature or the electric field shows the effect of the variant. Furthermore, repeated runs on the sample exhibit repeatable behaviour even though the absolute values of $C(f)$ and $G(f)$ may vary from one run to another. The peak value of the dielectric loss varies but it occurs at the same frequency (the relaxation frequency) and is independent of different runs. Most of the present analysis depends upon the relaxation frequency.

2.1. *Uncertainties of measurements*

The uncertainty in the measurement of C(100 Hz) in the range of 1 nF is about 2 per cent which decreases to 0·6 per cent for C(10 kHz) and 0·2 per cent for C(1 MHz). The uncertainty of G(100 Hz) is about 1·5 per cent and about 0·5 per cent for G(20 kHz) to G(1 MHz). The accuracy of the frequency is $\pm$20 ppm. Thus the accuracy of loss, $L(f)$, (equal to $\{G(f)/\omega\}$, where ω is the angular frequency) is primarily determined by the accuracy of $G(f)$. The relaxation frequencies which correspond to the peak value of the loss comes out to be $\pm$10 per cent for the loss in the range of 1–10 nF and $\pm$20 per cent in the range of 10–100 pF. The uncertainty in the temperature is $\pm$0·1°C.

2.2. *Theoretical evaluation of bulk parameters*

For the planar oriented ferroelectric sample in the frequency range of 100 Hz to 1 MHz, the possible relaxation mechanisms are the Goldstone mode and the soft mode. The molecular reorientations may contribute to the relaxation processes in the frequency range 10 MHz to 1 GHz. Levstik *et al.* [15] have shown that the dielectric strengths ($\Delta\varepsilon = \varepsilon(0) - \varepsilon(\infty)$) in the Goldstone mode ($\Delta\varepsilon_G$) and in the soft mode ($\Delta\varepsilon_s$) are given by

$$\Delta\varepsilon_G = (2\pi/K_\phi)\cdot(c\varepsilon/\mathbf{q}_0)^2 \tag{1a}$$

$$= (1/2\varepsilon_0 K_\phi)\cdot(P_s/\mathbf{q}_0 \sin(\theta))^2 \tag{1b}$$

and

$$\Delta\varepsilon_s = \{(\varepsilon c)^2/(\alpha(T - T_C) + (K_3 - \varepsilon\mu^2)\mathbf{q}_0^2)\}, \tag{2}$$

where K is the elastic constant and μ and c are the bilinear coupling coefficients of the flexoelectricity and the piezoelectricity. $\mathbf{q}_0 = (2\pi/Z_0)$ is the wave vector of the pitch Z_0 at the Curie temperature T_C. P_s is the spontaneous polarization and θ is the tilt angle. α is the coefficient contained in the temperature dependent term of the Landau expansion of the free energy density. In the vicinity of T_c, $\Delta\varepsilon_s$, may be approximated by neglecting the second term of the denominator in equation (2).

The complex dielectric constant $\varepsilon^*(\omega, T)$ for the symmetric distribution of the Cole–Cole type may be written as [16]

$$\varepsilon^*(\omega, T) - \varepsilon(\infty) = \frac{\Delta\varepsilon_G(T)}{1 + (j\omega\tau_G)^{1-h_G}} + \frac{\Delta\varepsilon_s(T)}{1 + (j\omega\tau_s)^{1-h_s}}, \tag{3}$$

where $\tau = 1/(2\pi f_r)$ is the relaxation time and h is the corresponding distribution parameter for the two modes. f_r is the relaxation frequency and $\varepsilon(\infty)$ is the high frequency limiting dielectric constant. The relaxation time in the Goldstone mode τ_G is given by

$$\tau_G = (\gamma_\phi/K_\phi \mathbf{q}_0{}^2), \tag{4}$$

where γ_ϕ is the coefficient of rotational viscosity. Combining equations (1) and (4) we get

$$\gamma_\phi = (1/4\pi\varepsilon_0)\cdot(P_s/\sin(\theta))^2\cdot(1/\Delta\varepsilon_G\cdot f_{rG}). \tag{5}$$

The elastic constant K_ϕ can also be calculated from equation (1).

For the soft mode, the relaxation frequency f_{rs} is

$$f_{rs} = [\alpha(T - T_C) + (K_3 - \varepsilon\mu^2)\mathbf{q}_0^2]/(2\pi\gamma_\theta). \tag{6}$$

From equations (2) and (6),

$$(\Delta\varepsilon_s\cdot f_{rs}) = (\varepsilon c)^2/(2\pi\gamma_\theta). \tag{7}$$

The coefficient of rotational viscosity γ_θ in the soft mode is inversely proportional to $(\Delta\varepsilon_s\cdot f_{rs})$.

2.3. *Analysis of experimental data*

The relaxation frequency f_r and the distribution parameter h may be calculated from the Cole–Cole equation [16] using

$$(v/u) = (\omega\tau)^{(1-h)} \tag{8}$$

where

$$v = [(\varepsilon(0) - \varepsilon'(\omega))^2 + (\varepsilon''(\omega))^2]^{1/2} \tag{9a}$$

and

$$u=[(\varepsilon'(\omega)-\varepsilon(\infty))^2+(\varepsilon''(\omega))^2]^{1/2}. \tag{9b}$$

Furthermore

$$\varepsilon'(\omega)=[C(f)-C(\text{air})]/C(L)$$

and $\varepsilon'(\omega)$ is proportional to $C(f)$ provided $C(\text{air})\ll C(f)$ which is true for the frequencies in the kHz region and $C(\text{L})$ is the live capacitance equal to $C(\text{air})-C(\text{stray})$. From the geometry of the parallel plate capacitor $C(\text{L})$ is estimated to be 18·4 pF. $\varepsilon''(\omega)=G(f)/\omega C(\text{L})$ where $G(f)$ is the measured conductance $\varepsilon''(\omega)$ is proportional to $G(f)/\omega$. A plot of $\log_{10}(v/u)$ against $\log_{10}(f)$ should give a straight line, the intercept on the abscissa axis corresponds to f_r and the slope gives the distribution parameter h. The data points may deviate from the straight line because at low frequencies, the value of (v/u) is very small as v is small and at high frequencies (v/u) is very large as u is small. This makes the value of $\log_{10}(v/u)$ very sensitive to the choice of $C(0)$ and $C(\infty)$.

An estimate of the DC conductivity due to the mobility of ions may be made from the measured conductance $G(f)$ using the Cole–Cole equation [17].

$$G(f)/\omega=G(\text{DC})/\omega+[A/\{\cosh\{(1-h)\ln(f/f_r)\}\sin(h\pi/2)\}], \tag{10}$$

where

$$A=\{C(0)-C(\infty)\}\cosh(h\pi/2)/2$$

is a constant. For the limiting case of h approaching zero, the above equation reduces to

$$G(f)/\omega=G(\text{DC})/\omega+\{(C(0)-C(\infty))\cdot\omega\tau/(1+\omega^2\tau^2)\}. \tag{11}$$

G(DC) has an appreciable effect at low frequencies and may even show a cusp in the Cole–Cole plot when $G(\text{DC})$ is comparable to $G(f)$. Taking $C(0)=C(100\text{ Hz})$, $C(\infty)=C(1\text{ MHz})$, h and f_r as obtained from equation (8), G(DC) could be estimated from the least square fit of the loss data using equation (10). The measured high frequency data in the MHz region may deviate from the true value, because we have not corrected for (i) the series lead inductance effect and (ii) the stray capacitance. However, these corrections do not affect the relaxation frequency f_r and the dielectric strength $\Delta\varepsilon$.

3. Results and discussion

3.1. *The Goldstone mode*

Figure 1 shows a typical graph for the dielectric loss $L(f)$ against $\log_{10} f$ at different temperatures for zero external DC bias. The relaxation frequency, f_r, of FLC#202 corresponds to the maximum loss. The peak value of the loss decreases with increasing temperature. At 58·6°C the dielectric loss peak disappears in this frequency range because the liquid crystal goes into the isotropic phase. The peak position is weakly temperature dependent and shifts to the higher frequencies with an increase in temperature of up to 50°C.

Figure 2 shows the Cole–Cole plots at various temperatures at zero DC bias. The points lie on a semicircle except for those at lower frequencies. The data at lower frequencies have been used to estimate the ionic conductance. The corrected points lie on the Cole–Cole arc (see figure 2, curves 1c, 2c etc.). At temperatures lower than 50°C, the static dielectric contstant $\varepsilon(0)$ almost corresponds to the capacitance at 100 Hz, whereas $\varepsilon(\infty)$ corresponds to the capacitance at 1 MHz. The data beyond 1 kHz do not change because of the ionic conductance and hence f_r remains unchanged.

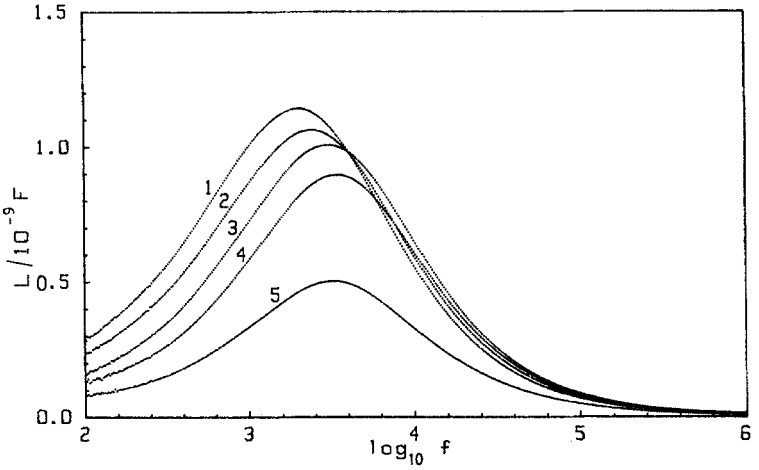

Figure 1. Dielectric loss versus $\log_{10} f$ at zero external DC field corresponding to the curve temperatures: (1) 30·2°C, (2) 34·8°C, (3) 44·3°C, (4) 48·8°C and (5) 53·6°C, respectively.

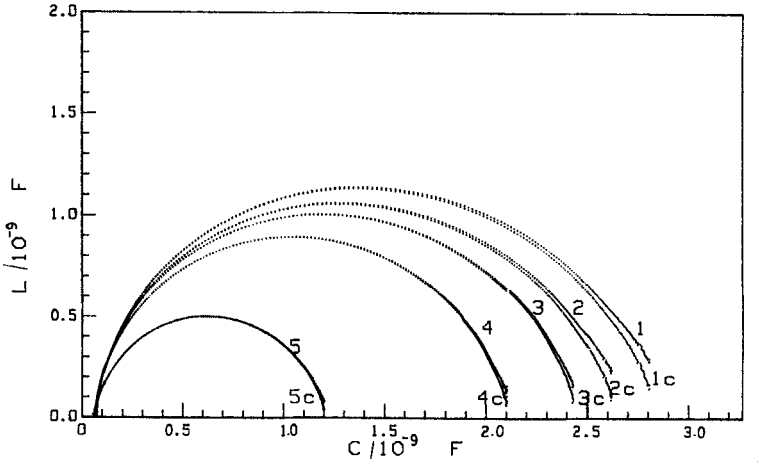

Figure 2. The Cole–Cole plots at zero external DC bias. The corresponding curve temperatures are: (1) 30·2°C, (2) 34·8°C, (3) 44·3°C, (4) 48·8°C and (5) 53·6°C, respectively.

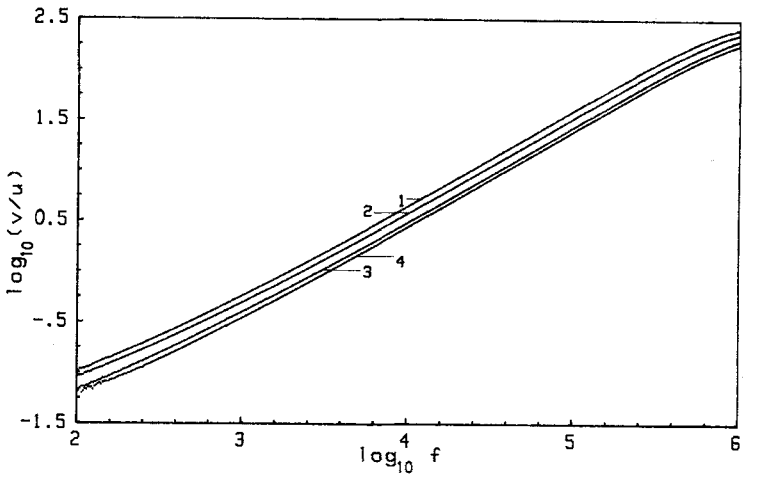

Figure 3. The plot of $\log_{10}(v/u)$ versus $\log_{10} f$ at zero external DC bias. The corresponding curve temperatures are: (1) 30·2°C, (2) 34·8°C, (3) 44·3°C and (4) 48·8°C, respectively.

The plot of $\log_{10}(v/u)$ versus $\log_{10} f$ is shown in figure 3. We see a deviation in the straight line behaviour on both the low and high frequency sides because of the reasons previously mentioned. However, around the intercept of the frequency axis, equation (8) becomes valid. Table 2 summarizes the results of f_r found from figures 3 and 1 and h from figure 3. The relaxation frequencies found from the two graphs are in good agreement confirming the validity of the Cole–Cole process of the dielectric relaxation in the liquid crystal. The value of h (about 0·10) does not show any significant change with temperature. So the number of relaxation mechanisms taking part in the process is the same in all cases. At lower temperatures, we also observe that f_r is almost equal to the frequency corresponding to the value of $[C(0)-C(\infty)]/2$ suggesting that the correction in $C(0)$ is negligible and also $C(0) \gg C(\infty)$. However, the loss becomes very low at high temperatures making the dielectric loss peak very broad and weak. Corrections in $C(f)$ become significant resulting in large uncertainties in f_r.

The temperature dependences of the dielectric strength ($\Delta\varepsilon$) and f_r in this material show three distinct regions: (i) 25 to 56°C, (ii) 56 to 58°C and (iii) above 58°C; above 58·4°C it goes into the isotropic phase. In the temperature range of 25 to 56°C $\Delta\varepsilon$ is proportional to $C(0)-C(\infty)$ and decreases with temperature (see figure 4). We find that the relaxation frequency of the Goldstone mode, f_{rG}, is not independent of temperature (see figure 5). On heating the material from 25 to 50°C, f_{rG} increases from 1·9 kHz to 3·5 kHz. On further heating from 50 to 56°C, f_{rG} decreases from 3·5 kHz to 2·8 kHz (see table 2). A similar behaviour has also been observed by Biradar *et al.* [5], though for their sample f_{rG} is only around 100 Hz. The Goldstone process is thus showing a temperature behaviour in which the relaxation frequency initially speeds up with temperature and then slows down near the S_C^*–S_A^* transition temperature.

Taking the tilt angle data from [14] and the spontaneous polarization data from [18], the rotational viscosity of the Goldstone mode γ_ϕ has been calculated using equation (5) and is plotted versus temperature in figure 6. The values of γ_ϕ lie between 0·03 and 0·05 Nsm^{-2} whereas the torsional viscosity coefficient for this mixture lies between 2 and 6 Nsm^{-2} in the temperature interval of 25 and 50°C (see [18]). The elastic constant K has been calculated taking the pitch data from [14] in equation (1); the values lie between 0·7 and $1{\cdot}6 \times 10^{-12}$ N in the temperature interval 30 to 55°C

Table 2. The values of the relaxation frequencies and their distribution parameters for FLC#202 at different temperatures for two typical DC fields.

T°C	Loss peak f_r kHz	Cole–Cole f_r kHz	Distribution parameter (h)
External applied DC electric field = 0 kV cm^{-1}			
28·0	1·9	1·8	0·11
30·0	2·0	1·9	0·12
34·8	2·4	2·3	0·12
38·8	2·8	2·6	0·13
44·3	3·0	2·9	0·12
48·8	3·4	3·3	0·10
50·0	3·5	3·4	0·11
51·8	3·4	3·4	0·11
52·9	3·3	3·3	0·11
53·6	3·2	3·2	0·10
54·8	3·0	3·0	0·10
55·6	2·8	2·8	0·10
56·6	6·8	6·6	0·08
57·5	37	37	0·08
External applied DC electric field = 5·66 kV cm^{-1}			
28·0	2·8	2·7	0·10
30·0	2·9	2·8	0·11
35·0	3·4	3·3	0·11
39·8	3·9	3·7	0·12
41·9	4·1	3·9	0·12
44·3	4·0	3·9	0·12
46·2	4·0	3·8	0·12
48·5	4·3	3·9	0·14
50·7	4·2	4·1	0·19
51·6	4·2	4·2	0·22
52·2	4·2	4·3	0·22
53·0	4·2	4·3	0·30
54·1	4·0	4·1	0·37
56·8	19	17	0·13
57·7	38	37	0·06

which are of the same order of magnitude as for 4-(2-methylbutyloxy)phenyl 4-*n*-decyloxybenzoate [8]. The variation of K with temperature is shown in figure 7. We find that $R = (P_s/\sin(\theta))^2/\Delta\varepsilon_G$ remains constant for the material with temperature for a given electric field (see table 3). The temperature dependence of $\Delta\varepsilon_G$ is, therefore, due to the temperature dependence of P_s and θ. The variation of the elastic constant with temperature may, therefore be due to the temperature dependence of the pitch Z (see equation (1 *b*)). It may be emphasized that equations (1) and (5) are valid only for the S_C^* phase and any attempt to calculate γ and K for the S_A^* phase based on this model may lead to erroneous results as indicated by the abrupt jumps in figures 6 and 7 at 55°C.

3.2. *Effect of external DC bias*

3.2.1. *Goldstone mode in weak electric field*

In the temperature range 25 to 50°C the capacitance at 100 Hz shows a slight increase with increasing electric field up to 2 kV cm^{-1}, thereby suggesting that the orientation of the electric dipoles is along the direction of the weak applied electric field

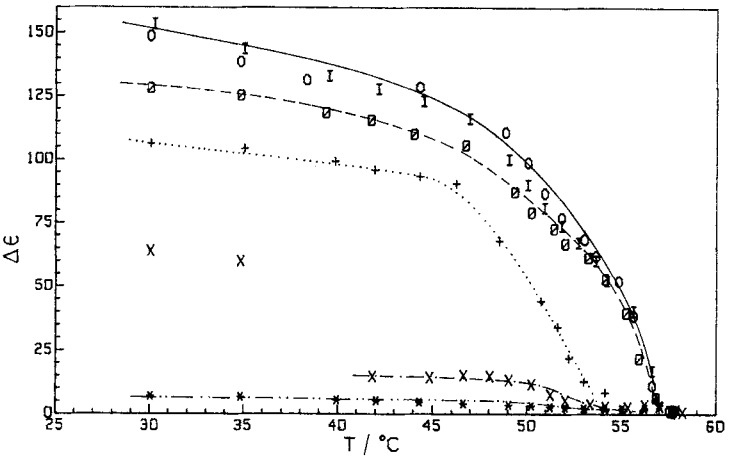

Figure 4. The plot of the dielectric strength versus temperature at different DC fields: (0) 0 kV cm^{-1}, (I) 1·89 kV cm^{-1}, (Ø) 3·77 kV cm^{-1}, (+) 5·66 kV cm^{-1}, (×) 6·60 kV cm^{-1} and (*) 9·43 kV cm^{-1}, respectively.

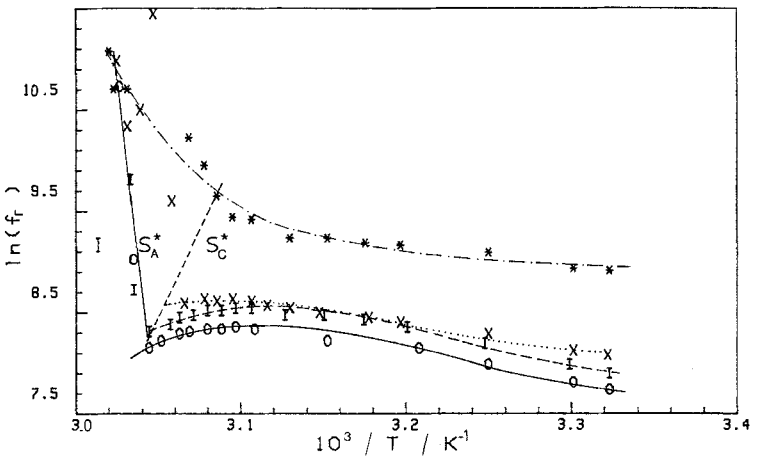

Figure 5. ln (f_r) versus temperature for different DC fields: (0) 0 kV cm^{-1}, (I) 1·89 kV cm^{-1} (×) 5·66 kV cm^{-1} and (*) 9·43 kV cm^{-1}, respectively.

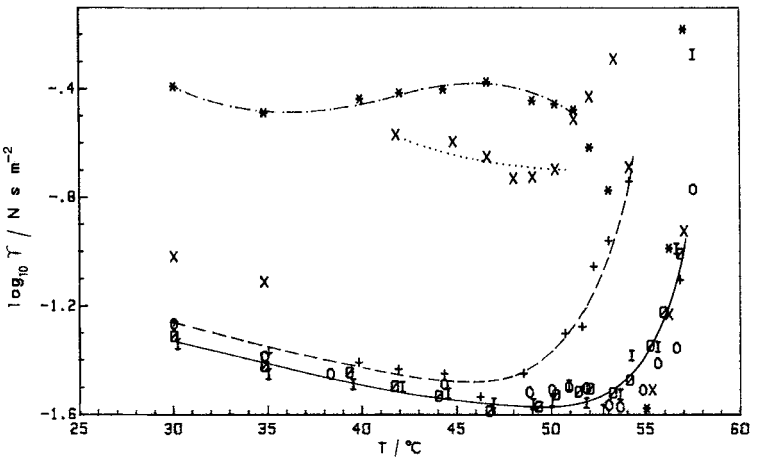

Figure 6. The plot of $\log_{10}\gamma$ versus temperature at different DC fields: (0) 0 kV cm^{-1}, (I) 1·89 kV cm^{-1}, (Ø) 3·77 kV cm^{-1}, (+) 5·66 kV cm^{-1}, (×) 6·60 kV cm^{-1} and (*) 9·43 kV cm^{-1}, respectively.

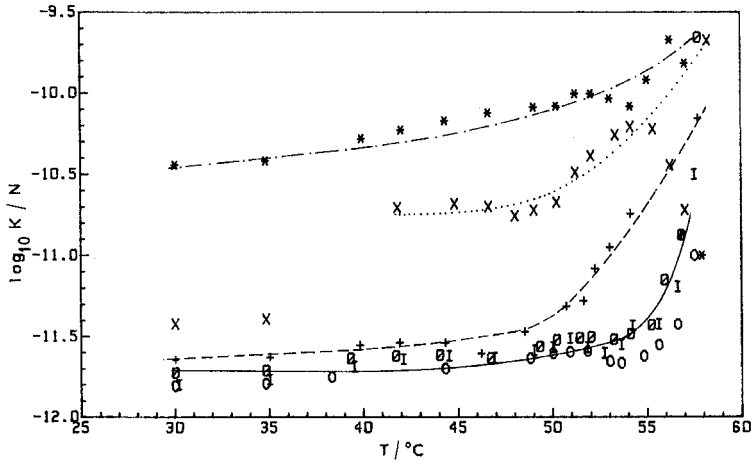

Figure 7. The plot of $\log_{10}K$ versus temperature at different DC fields: (0) 0 kV cm^{-1}, (I) 1·89 kV cm^{-1}, (Ø) 3·77 kV cm^{-1}, (+) 5·66 kV cm^{-1}, (×) 6·60 kV cm^{-1} and (*) 9·43 kV cm^{-1}, respectively.

Table 3. The calculated values of $R = (P_s \sin\theta)^2/\Delta\varepsilon_G$ for the Goldstone mode at different electric fields.

E/kV cm^{-1}	$R \times 10^{-4}$
0·00	1·11 ± 0·08
1·89	1·15 ± 0·10
3·77	1·22 ± 0·08
5·66	1·52 ± 0·28
6·60	10·2 ± 1·5
9·43	33·7 ± 6·0

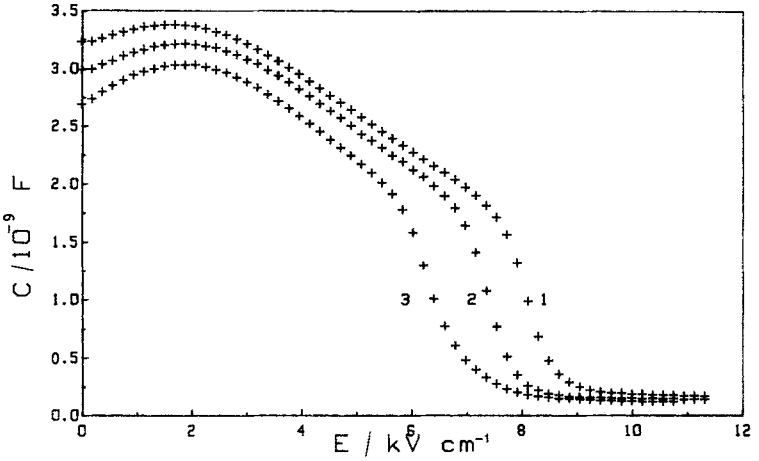

Figure 8. The capacitance at 100 Hz versus the external DC field at different temperatures. The corresponding curve temperatures: (1) 25·0°C, (2) 34·8°C and (3) 44·3°C, respectively.

(see figure 8). The relaxation frequencies decrease slightly with electric field in this range. The variation of the relaxation frequency with DC electric field at different temperatures is shown in figure 9. The relaxation frequency is very weakly dependent on the electric field up to 5·7 kV cm^{-1}. On increasing the DC electric field from 2 to 6·5 kV cm^{-1}, the dipole moments are strongly oriented and become parallel to the applied field; this results in the decrease of the dielectric permittivity since the dipoles are now almost unable to follow the alternating measuring electric field (see figure 4). The molecular tilt angle depends strongly on the temperature. However, the distribution of the azimuthal angle of the molecular plane in a helicoidal ferroelectric liquid crystal begins to become distorted from its sinusoidal distribution above a DC field of 2 kV cm^{-1}. Here, this effect manifests itself in the form of an increase in f_r with increasing temperature and electric field (see figure 9). The rotational viscosity and elastic constants are calculated from equations (5) and (1) at these fields and the calculated values are shown in figures 6 and 7. The viscosity and the elastic constant are almost invariant with field up to 5·7 kV cm^{-1} since the S_C^* helix is not yet unwound. The parameter R increases with electric field (see table 3) but remains unchanged with temperature. The spontaneous polarization P_s increases with electric field until the helical structure is no longer completely unwound. Above the critical field E_c, P_s becomes independent of the electric field (E) [18]. The increase in R with electric field in the S_C^* phase may, therefore, be due to an increase of P_s with electric field. It may be noted that the standard deviation in R increases from 8 to 18 per cent at higher fields.

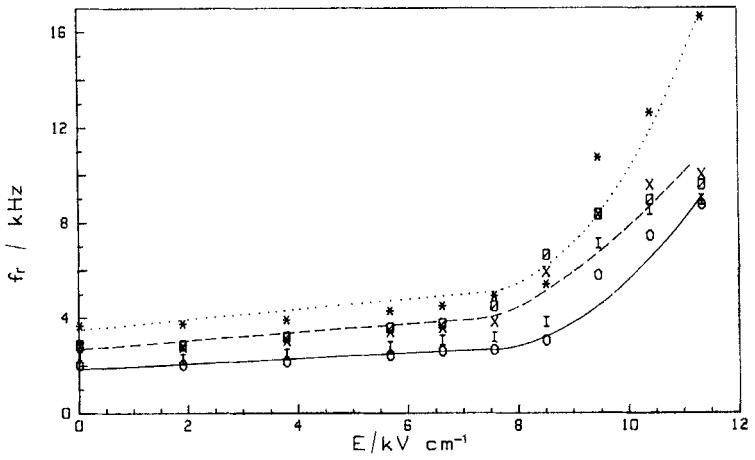

Figure 9. The relaxation frequency versus DC field at different temperatures: (0) 25·0°C, (I) 30·2°C, (×) 34·8°C, (Ø) 38·8°C and (*) 48·8°C, respectively.

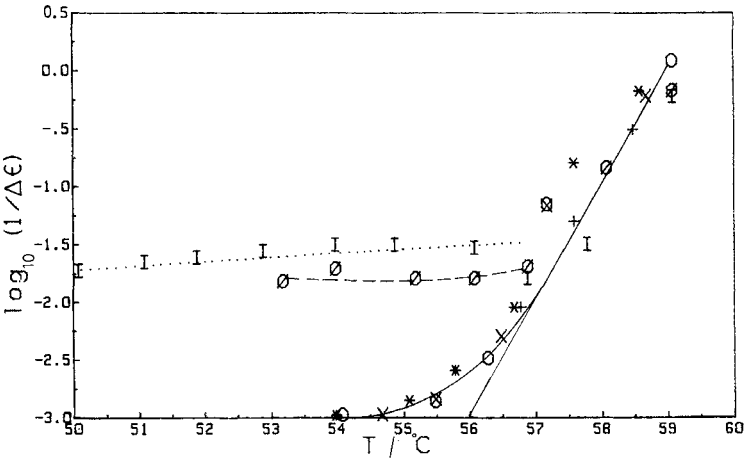

Figure 10. The plot of $\log_{10}(1/\Delta\varepsilon)$ versus temperature at different DC fields: (×) 0 kV cm^{-1}, (0) 1·89 kV cm^{-1}, (*) 3·77 kV cm^{-1}, (+) 5·66 kV cm^{-1}, (Ø) 6·60 kV cm^{-1} and (I) 9·43 kV cm^{-1}, respectively.

3.2.2. *Soft mode in weak electric field*

In the S_C^* phase upto 56°C, we could not observe the soft mode because $1/\Delta\varepsilon$ and f_r are only weakly temperature dependent and both parameters do not behave critically on the transition temperature T_C [9]. There is a slight decrease in the relaxation frequency in the temperature range 50 to 56°C up to an electric field of 5·6 kV cm^{-1}. However, the decrease is marginal and cannot be assigned to the soft mode. At 55·9°C a distorted Cole–Cole plot is obtained; it is difficult to resolve it into the Goldstone mode, the soft mode and the contribution of the ionic conductivity. On increasing the temperature from 56 to 58°C there is once again a single loss peak and Cole–Cole arc after correcting the data for the ionic conductance as discussed earlier. The relaxation frequency depends critically on the temperature with T_C equal to 56·1°C (see figure 5). The slope of the relaxation frequency is +25·2 kHz °C^{-1}, a value very close to that of LC1 [9].

$\Delta\varepsilon$ decreases with increasing temperature. The plot of $\log_{10}(1/\Delta\varepsilon)$ versus temperature is shown in figure 10; it deviates from the straight line behaviour near the S_C^*–S_A^* temperature although it approaches critically to 56·0°C. Therefore FLC#202 undergoes an S_C^*—S_A^* transition at 56·1°C as observed from the temperature dependence of $1/\Delta\varepsilon_s$ and f_{rs}. The parameter R is not constant in the S_A^* phase and increases with temperature for all DC fields.

3.2.3. *Strong field*

When the DC electric field is increased above 6·5 kV cm^{-1} at a fixed temperature below 50°C, there is an abrupt drop in the capacitance (see figure 8). At this field the helix is completely unwound and the sample goes from the twisted S_C^* phase to the unwound S_C^* phase. This critical field is close to the field of 5·6 kV cm^{-1} obtained by Beresnev *et al.* [13]. The capacitance at a field greater than the critical field is almost independent of the applied field. The critical field from the measurement of capacitance shows a very small frequency dependence between 100 Hz and 500 Hz, viz. its value at 25°C changes from 7·4 kV cm^{-1} at 100 Hz to 7·7 kV cm^{-1} at 500 Hz. The critical field decreases with temperature at a given frequency, viz. at 100 Hz it is 7·4 kV cm^{-1} at 25°C, 6·6 kV cm^{-1} at 35°C, 6·0 kV cm^{-1} at 40°C and 5·7 kV cm^{-1} at 45°C. However, Beresnev *et al.* [13] observe a strong frequency dependence on the critical field for this material on applying a square wave voltage in their electrooptical experiments.

The unwound helical structure shows two distinct temperature regions for $\Delta\varepsilon$ and f_r at 9·4 kV cm^{-1}; region I: 25 to 50°C and region II: 50 to 58°C (see figures 5 and 10, respectively). In region I (the unwound S_C^* phase) f_r and $1/\Delta\varepsilon$ are very weakly temperature dependent. In region II (50 to 58°C at 9·4 kV cm^{-1}, the unwound S_A^* phase) $1/\Delta\varepsilon$ changes slowly with temperature up to 56°C and then suddenly rises (see figure 10).

4. Conclusions

The dielectric constant of FLC#202 in the S_C^* phase follows the same temperature behaviour as that of $(P_s/\sin\theta)^2$. From the critical behaviour of dielectric strength and relaxation frequency the material shows the following phase transitions:

$$S_C^* \ 56{\cdot}1°C \ S_A^* \ 58°C \ I.$$

The relaxation frequency of the Goldstone mode of this material is 2 kHz at 30°C, which is the highest of all ferroelectric liquid crystals studied so far. We could not observe the soft mode in the S_C^* phase, but it was observed in the S_A^* phase.

The critical field necessary to unwind the helix has been measured by observing an abrupt jump in the capacitance and this field decreases with temperature. The phase transitions under the strong electric field are found to be

$$S_C^* \text{ (unwound) } 50°C\ S_A^* \text{ (unwound) } 58°C\ I.$$

The temperature for the unwound transition S_C^*–$S_A^*(T_{S_C^*S_A^*})$ decreases with applied DC field.

This material may, therefore, be quite suitable for electrooptical applications because besides having a large spontaneous polarization and a small pitch, it has a very high relaxation frequency at room temperature.

We thank the University Grants Commission, New Delhi for a COSIST programme grant.

References

[1] BERESNEV, L. A., BLINOV, L. M., OSIPOV, M. A., and PIKIN, S. A., 1988, *Molec. Crystals Liq. Crystals* A, **158,** 3.
[2] MINAMI, N., and TAKANO, S., 1988, *Molec. Crystals. liq. Crystals*, **5,** 187.
[3] EZCURRA, A., PEREZ JUBINDO, M. A., DELA FUENTE, M. R., ETXEBARRIA, J., SERRANO, J. L., and MARCUS, M., 1988, *Ferroelectrics*, **81,** 1369.
[4] PAVEL, J., GLOGAROVA, M., and DABROWSKI, R., 1988, *Ferroelectrics*, **81,** 1377.
[5] BIRADAR, A. M., WROBEL, S., and HASSE, W., 1989, *Phys. Rev.* A, **39,** 2693.
[6] FILIPIC, C., CARLSSON, T., LEVSTIK, A., ZEKS, B., BLINC, R., GOUDA, F., LAGERWALL, S. T., and SKARP, K., 1988, *Phys. Rev.* A, **38,** 5833.
[7] GOUDA, F., ANDERSSON, G., CARLSSON, T., LAGERWALL, S. T., SKARP, K., and STEBLER, B., 1989, *Molec. Crystals Liq. Crystals Lett.*, **6,** 151.
[8] GOUDA, F., SKARP, K., ANDERSSON, G., KRESSE, H., and LAGERWALL, S. T., 1989, *Jap. J. appl. Phys.*, **28,** 1887.
[9] GOUDA, F., SKARP, K., and LAGERWALL, S. T., 1989, *Proceedings 2nd International Conference on Ferroelectric Liquid Crystals*, Goteborg.
[10] GOUDA, F., ANDERSSON, G., LAGERWALL, S. T., SKARP, K., STEBLER, B., CARLSSON, T., FILIPIC, C., ZEKS, B., and LEVSTIK, A., 1989, *Liq. Crystals*, **6,** 219.
[11] GLOGAROVA, M., LEJCEK, L., PAVEL, J., JANOVEC, V., and FOUSEK, J., 1982, *Czech. J. Phys.* **32,** 943.
[12] BAWA, S. S., BIRADAR, A. M., and CHANDRA, S., 1987, *Jap. J. Appl. Phys.*, **26,** 189.
[13] BERESNEV, L. A., BLINOV, L. M., DERGACHEV, D. I., and KONDRAT'EV, S. B., 1987, *JETP Lett.*, **46,** 413.
[14] BERESNEV, L. A., BLINOV, L. M., and DERGACHEV, D. I., 1988, *Ferroelectrics*, **85,** 173.
[15] LEVSTIK, A., CARLSSON, T., FILIPIC, C., LEVSTIK, I., and ZEKS, B., 1987, *Phys. Rev.* A, **35,** 3527.
[16] HILL, N. E., VAUGHAN, W. E., PRICE, A. H., and DAVIES, M., 1969, *Dielectric Properties and Molecular Behaviour*, (Van-Nostrand Reinhold Co.), p. 290.
[17] BOTTCHER, C. J. F., and BORDEWIJK, P., 1978, *Theory of Electric Polarization*, Vol. 2 (Elsevier), p. 62.
[18] SRIVASTAVA, S. L., (unpublished data).